Models for the integer quantum Hall effect: The network model, the Dirac equation, and a tight-binding Hamiltonian

C.-M. Ho and J.T. Chalker
Theoretical Physics, University of Oxford, 1, Keble Road, Oxford OX1 3NP, United Kingdom
(Received 19 April 1996)

We consider models for the plateau transition in the integer quantum Hall effect. Starting from the network model, we construct a mapping to the Dirac Hamiltonian in two dimensions. In the general case, the Dirac Hamiltonian has randomness in the mass, the scalar potential, and the vector potential. Separately, we show that the network model can also be associated with a nearest-neighbor, tight-binding Hamiltonian. [S0163-1829(96)05935-8]

I. INTRODUCTION

Anderson localization is central to understanding the integer quantum Hall effect (IQHE).[1] In particular, the plateau transitions between different quantized values for the Hall conductance reflect delocalization transitions in each Landau level. Scaling ideas[2] provide a framework for understanding these transitions, and are supported by the results of experiment[3] and of numerical simulation.[1] Progress toward an analytical theory of the critical point, however, remains limited.

The simplest starting point for such a theory is to neglect electron-electron interactions and consider a single particle moving in a magnetic field with a disordered impurity potential. In a pioneering work, Pruisken and collaborators[4] obtained from this a field-theoretic description in terms of a σ model. More recently, in response to the difficulties of extracting quantitative results from the σ model, several alternative formulations have been explored: Read,[5] Lee,[6] and Zirnbauer[7] have investigated spin chains; Lee and Wang[8] have considered the replica limit of Hubbard chains; and Ludwig and collaborators[9] have discussed the Dirac equation.

The correspondence between Dirac fermions in two space dimensions, and nonrelativistic charged particles moving in a magnetic field, stems from the fact that time-reversal symmetry is broken both by a mass term in the two-dimensional Dirac equation[9,10] and by a magnetic field in the Schrödinger equation. Moreover, as emphasized by Ludwig *et al.*, the Hall conductance of Dirac fermions, with fixed Fermi energy, has a jump of e^2/h if the fermion mass is tuned through zero. The critical behavior at this transition depends on the symmetries of the Hamiltonian. The Dirac equation with only a random vector potential is particularly amenable to analysis[9,11] since the zero-energy eigenstates are known explicitly.[12] Critical properties are controlled by a line of fixed points, and turn out to be different from those expected at the plateau transitions in the IQHE. The line of fixed points, however, is unstable against additional randomness, either in the mass or in the scalar potential, and flow is conjectured[9] to be towards a generic quantum Hall fixed point, describing the same critical behavior as emerges from the usual Schrödinger equation.

Confidence that Dirac fermions with suitable randomness do indeed have a critical point in the same universality class as the IQHE plateau transitions is clearly strengthened if there exists an explicit mapping from a microscopic model for the IQHE to the Dirac Hamiltonian. Fisher and Fradkin,[13] and subsequent authors,[9,15] have reached the Dirac equation starting from certain, rather specific, tight-binding models. An alternative to the tight-binding model, as a description of the IQHE, is the network model,[16] studied extensively by numerical simulation.[17] Ludwig and collaborators[9] have asserted that Dirac fermions with various possible kinds of randomness each represent particular forms of the network model. These authors, however, did not set out a transformation from one model to the other. Separately, Lee[6] found such a transformation in the particular case of a network model without random phases, obtaining Dirac fermions with randomness only in the mass.

The purpose of this paper is to describe a general mapping from the network model to the Dirac Hamiltonian in two dimensions, which, in the unrestricted case, has randomness in the mass, the scalar potential, and the vector potential. Any approach to this problem must confront the fact that the network model is defined using the language of scattering theory, and therefore, at least in the first instance, contains information only about behavior at one energy. The Dirac Hamiltonian, by contrast, obviously fixes properties of an entire spectrum of eigenstates. We begin from a unitary matrix defined[19] for the network model, which, heuristically, can be thought of as a time-evolution operator. We show, in a continuum limit, that it is the evolution operator for a Dirac Hamiltonian. In this respect, our route is rather different from that of Lee,[6] who obtains a Hamiltonian by endowing the phases of the network model with an energy dependence. We also differ in taking the continuum limit isotropically, while Lee[6] does so anisotropically.

Our mapping is described in Sec. II. In Sec. III we examine in detail how edge states of the network model are related to boundary states of Dirac fermions. This is important, since it is these states that are responsible for the quantized Hall conductance away from plateau transitions.

Equivalence between the network model and the Dirac Hamiltonian necessarily requires a continuum limit. In Sec. IV, we show that, independently of the continuum limit, one

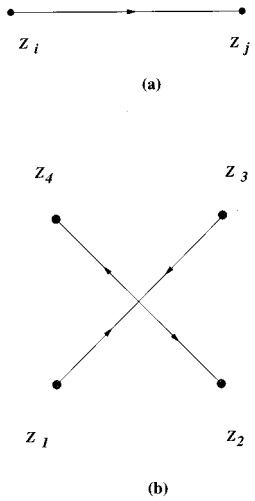

FIG. 1. Components of the network model: links (a) and nodes (b).

can associate with the network model a tight-binding Hamiltonian, which contains only nearest-neighbor hopping.

II. MAPPING FROM THE NETWORK MODEL TO THE DIRAC HAMILTONIAN

In this section we construct an explicit mapping from the network model[16] to the Dirac Hamiltonian in two dimensions. First, we recall the physical basis for the network model and its definition. Consider nonrelativistic, charged particles moving in a smoothly varying scalar potential in two dimensions, with a strong perpendicular magnetic field. The potential is smooth if its correlation length is much larger than the cyclotron radius, and the field is strong if the cyclotron energy is larger than the amplitude of potential fluctuations. Under these conditions, the kinetic energy of cyclotron motion about the guiding center, and the potential energy associated with the position of the guiding center, are both separately conserved. We focus on drift of guiding centers along equipotential lines. In the network model, portions of a given equipotential are represented by directed ''links,'' and the wave function for the particle is represented by complex current amplitudes Z, defined at points on each link. On traversing a link, a particle aquires an Aharonov-Bohm phase: if Z_i and Z_j are amplitudes at opposite ends of the link k [see Fig. 1(a)], $Z_j = e^{i\phi_k} Z_i$. Tunneling between two disjoint portions of the equipotential can occur where they are separated by less than a cyclotron radius, as happens near saddle points in the potential. It is incorporated into the model at ''nodes,'' where two incoming and two outgoing links meet. The amplitudes on the four links that meet at a given node may be related by a transfer matrix or by a scattering matrix. In a suitable gauge, each of these 2×2 matrices is real and depends on a single parameter, which we denote by θ (for the transfer matrix) and β (for the scattering matrix). The parameter determines the relative probabilities for a particle to turn to the left or to the right on arriving at the node. It is a smooth function of the equipotential energy, measured relative to the potential at the saddle point.[18] Referring to Fig. 1(b), one has

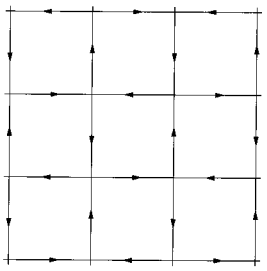

FIG. 2. The network model on a square lattice.

$$\begin{pmatrix} Z_4 \\ Z_3 \end{pmatrix} = \begin{pmatrix} \cosh\theta & \sinh\theta \\ \sinh\theta & \cosh\theta \end{pmatrix} \begin{pmatrix} Z_1 \\ Z_2 \end{pmatrix} \tag{1}$$

and

$$\begin{pmatrix} Z_2 \\ Z_4 \end{pmatrix} = \begin{pmatrix} \cos\beta & \sin\beta \\ -\sin\beta & \cos\beta \end{pmatrix} \begin{pmatrix} Z_1 \\ Z_3 \end{pmatrix}. \tag{2}$$

The two parameters are related by $\sin\beta = -\tanh\theta$. On varying the equipotential energy from far below that of the saddle point to far above, β increases from $\beta = 0$ to $\beta = \pi/2$; tunneling is a maximum at $\beta_c = \pi/4$.

The network model as a whole is built by connecting these two elements—links and nodes—to form a lattice. The simplest choice is the square lattice, illustrated in Fig. 2. Randomness is introduced by choosing each link phase ϕ_k independently from a probability distribution. The model represents particle motion at an energy determined by the value of the node parameters. If all nodes are identical, and if phases are uniformly distributed between 0 and 2π, the system is critical at $\beta = \beta_c$, and in the localized phase otherwise.

We follow Klesse and Metzler,[19] and associate a unitary matrix with the model. Roughly speaking, this matrix is a time evolution operator. Let the unit of time be the interval required for a guiding center to drift from the midpoint of one link, through a node, to the midpoint of the next link; ignore dispersion in this time interval, arising from variations in drift velocity or in lengths of links. Let $Z(\mathbf{r};L)$ be the amplitude for a particle to arrive at a point $\mathbf{r}$ after L time steps, starting from an initial wave function $Z(\mathbf{r}';0)$. Then

$$Z(\mathbf{r};L+1) = \sum_{\mathbf{r}'} T_{\mathbf{r},\mathbf{r}'} Z(\mathbf{r}';L), \tag{3}$$

and T is the required time evolution operator. Eigenfunctions of T with eigenvalue 1 are stationary states of the network model.

In Eq. (3), the element $T_{\mathbf{r},\mathbf{r}'}$ is nonzero only if there is a one-step path on the lattice from $\mathbf{r}$ to $\mathbf{r}'$: that is, a path that follows the directions of the links and passes only one node. The values of these nonzero elements are given[19] by a product of a phase factor from the link traversed, and a tunneling amplitude from the node, with sign conventions indicated in Fig. 3.

To be definite, consider the system illustrated in Fig. 4. Plaquettes are labeled by the coordinates, (x,y), of their centers. With our choice of lattice constant and of orientation for the axes, (x,y) are a pair of integers, either both even or both

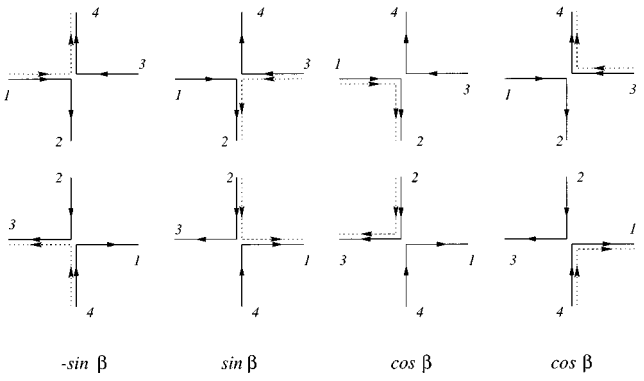

FIG. 3. Amplitudes associated with possible scattering paths at nodes.

odd. We denote the four links i making up a plaquette by $i=1,\ 2,\ 3$ and 4, so that a point $\mathbf{r}$ on the network is specified by the combination (x,y,i). Initially, we take the tunneling parameter β to be the same at every node, and the four phases ϕ_i to be the same on every plaquette. In addition, it is convenient to measure the phases relative to their value when half a flux quantum threads each plaquette, by replacing ϕ_4 with $\phi_4+\pi$.

Because each plaquette has four links, the matrix T has a 4×4 block structure, and because the midpoints of links form a bipartite lattice, each such block consists of two 2×2 blocks. To exhibit this structure, we arrange the amplitudes $Z(\mathbf{r};L)\equiv Z_i(x,y;L)$ in the order (Z_+,Z_-), with $Z_+(x,y)=(Z_1(x,y),Z_3(x,y))$ and $Z_-(x,y)=(Z_2(x,y),Z_4(x,y))$, suppressing the time L for clarity. In this basis, the evolution operator is

$$T=\begin{pmatrix}0 & M\\ N & 0\end{pmatrix}, \tag{4}$$

where

$$M=\begin{pmatrix}Se^{i\phi_1}t_-^x t_+^y & Ce^{i\phi_1}\\ Ce^{i\phi_3} & -Se^{i\phi_3}t_+^x t_-^y\end{pmatrix} \tag{5}$$

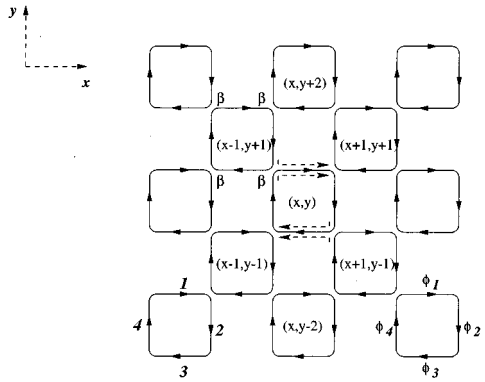

FIG. 4. The network model, showing (i) our coordinate system for plaquettes; (ii) labeling of the four links that make up a plaquette; and (iii), with dashed lines, the paths that contribute to $Z_i(x,y;L+1)$ for $i=1,3$.

and

$$N=\begin{pmatrix}Ce^{i\phi_2} & Se^{i\phi_2}t_+^x t_+^y\\ Se^{i\phi_4}t_-^x t_-^y & -Ce^{i\phi_4}\end{pmatrix}. \tag{6}$$

Here, we have introduced the abbreviations $C=\cos\beta$ and $S=\sin\beta$, and the translation operators, $t_\pm^x$ and $t_\pm^y$, defined by their action, $t_\pm^x Z_i(x,y)=Z_i(x\pm1,y)$ and $t_\pm^y Z_i(x,y)=Z_i(x,y\pm1)$. The first row of M, for example, expresses the fact, illustrated in Fig. 4, that $Z_1(x,y;L+1)=Se^{i\phi_1}Z_2(x-1,y+1;L)+Ce^{i\phi_1}Z_4(x,y;L)$.

In order to decouple Z_+ from Z_-, we consider the two-step evolution operator,

$$W\equiv T^2=\begin{pmatrix}MN & 0\\ 0 & NM\end{pmatrix}. \tag{7}$$

We may then deal just with the upper-left block, $U\equiv MN$, in the matrix W, and the component-pair Z_+. Since, at this stage, we are treating a system without disorder, U is diagonalized by a Fourier transform. We write its eigenvectors $\mathbf{u}$ as $\mathbf{u}^\top(x,y)=(v,w)e^{i(q_x x+q_y y)}$ and find

$$U\mathbf{u}=e^{-iV}\begin{pmatrix}\gamma & \alpha\\ -\alpha^* & \gamma^*\end{pmatrix}\mathbf{u}=e^{i(\chi-V)}\mathbf{u}, \tag{8}$$

where

$$V=-\frac{1}{2}\sum_{j=1}^{4}\phi_j,$$

$$\gamma=2SCe^{i[1/2\,(\phi_1-\phi_3)-q_x]}\cos[\tfrac{1}{2}\,(\phi_2-\phi_4)+q_y], \tag{9}$$

$$\alpha=e^{i[1/2\,(\phi_1-\phi_3)+q_y]}[S^2e^{i[1/2\,(\phi_2-\phi_4)+q_y]}-C^2e^{-i[1/2\,(\phi_2-\phi_4)+q_y]}],$$

and γ^*, α^* are the corresponding complex conjugates. The eigenvalues of U are $e^{i(\chi-V)}$ with a phase χ given by

$$\cos\chi\equiv\sin2\beta\cos(q_x-A_x)\cos(q_y-A_y), \tag{10}$$

in which $A_x=(\phi_1-\phi_3)/2$ and $A_y=(\phi_4-\phi_2)/2$. Setting $\beta=\beta_c+m/2\equiv\pi/4+m/2$, and taking $-\pi\leqslant\chi<\pi$, the range of allowed values for χ has gaps around $\chi=0$ and $\chi=\pm\pi$ for $m\neq0$: χ satisfies $-\pi+|m|\leqslant\chi\leqslant-|m|$ or $|m|\leqslant\chi\leqslant\pi-|m|$. This dispersion relation is illustrated in Fig. 5. Stationary states of the network model are characterized by $\chi-V=0$.

To extract from the unitary evolution operator a Dirac Hamiltonian H, we write $U=e^{-i\widetilde{H}}$ and work in the continuum limit, in which $\widetilde{H}$ is small. Thus we expand around $(q_x,q_y)=(0,0)$, taking m and the link phases ϕ_j to be small. To leading order, Eq. (10) gives the spectrum

$$\chi^2=m^2+(q_x-A_x)^2+(q_y-A_y)^2 \tag{11}$$

for small χ. At an operator level, when $t_\pm^x$ and $t_\pm^y$ act on smooth functions we make the replacements $t_\pm^x=1\pm\partial_x$ and $t_\pm^y=1\pm\partial_y$. Then

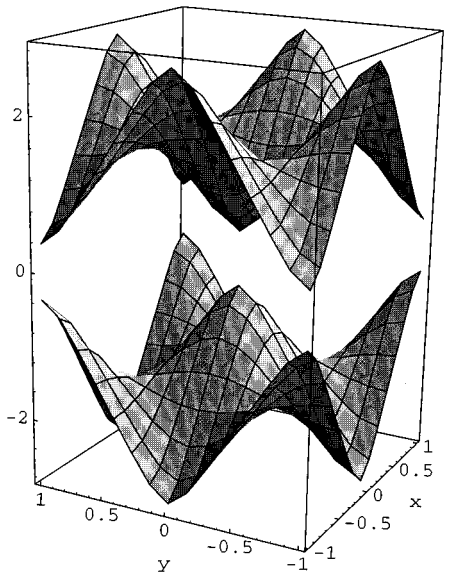

FIG. 5. The dispersion of χ (vertical axis) plotted as a function of $(p-A)_x$ and $(p-A)_y$ (horizontal plane) in units of π. The width of the gap between the two bands is determined by the mass, which is 1.2 here.

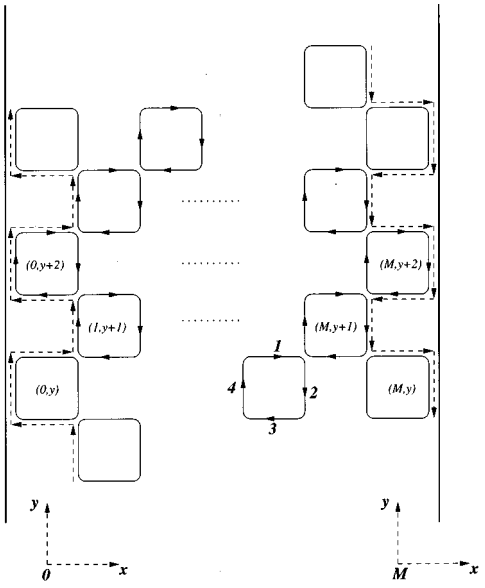

FIG. 6. The network model defined on a strip of width M. Dashed arrows indicate the propagation direction of edge states. The dotted arrow represents the boundary condition, Eq. (17).

$$U \approx 1 + \begin{pmatrix} -\partial_x + iA_x & \partial_y - iA_y + m \\ \partial_y - iA_y - m & \partial_x - iA_x \end{pmatrix} - iV \equiv 1 - i\tilde{H}. \tag{12}$$

Finally, to bring the Hamiltonian into a conventional form, we make a rotation in the two-component space, setting $H = G\tilde{H}G^{-1}$, with

$$G = \frac{1}{\sqrt{2}} \begin{pmatrix} i & -1 \\ i & 1 \end{pmatrix} \tag{13}$$

and obtain

$$H = (p_x - A_x)\sigma_x + (p_y - A_y)\sigma_y + m\sigma_z + V, \tag{14}$$

where $p_x = -i\partial_x$, and similarly for p_y, and we use the Pauli matrix representation

$$\sigma_x = \begin{pmatrix} 0 & 1 \\ 1 & 0 \end{pmatrix}, \quad \sigma_y = \begin{pmatrix} 0 & -i \\ i & 0 \end{pmatrix}, \quad \sigma_z = \begin{pmatrix} 1 & 0 \\ 0 & -1 \end{pmatrix}. \tag{15}$$

Now consider a network model with randomness. If the link phases and tunneling parameter vary smoothly in space, one obtains in the continuum limit the Dirac Hamiltonian, Eq. (14), with randomness in the vector potential, scalar potential, and mass. Specifically, fluctuations in the vector potential **A** arise from randomness in the individual link phases, fluctuations in the scalar potential V come from variations in the total Aharonov-Bohm phase associated with each plaquette, and fluctuations in the mass m are present if the tunneling parameter is not constant everywhere. The time-independent states of the network model correspond to the zero-energy states of the Dirac Hamiltonian.

This mapping can also be carried through for generalizations of the network model. In particular, the two-dimensional model in which each link carries N channels[16] is equivalent to the $U(N)$ Dirac Hamiltonians investigated by Fradkin.[14]

III. EDGE STATES IN THE NETWORK MODEL AND THE DIRAC EQUATION

The edge of a sample is, of course, set by a scalar confining potential in the usual description of the IQHE, based on the Schrödinger equation. Dirac fermions, by contrast, are confined by a spatially dependent mass, as discussed by Ludwig *et al.*[9] In particular, chiral, zero-energy states of Dirac fermions are associated with contours of zero mass.[9] We discuss in this section how such edge states emerge in our mapping from the network model to the Dirac Hamiltonian.

Consider a network model defined on a strip of finite width, as in Fig. 6. For energies in the lower half of the Landau level, corresponding to values of the node parameter $\beta < \beta_c$, all states are localized, while for energies in the upper half of the Landau level, for which $\beta > \beta_c$, a pair of extended states appears, one at each edge of the strip.[16]

The evolution operator U acting on the two-component wave function, $Z_+(L)$, introduced for the bulk of the system in the preceding section, is supplemented at the edge by the following boundary conditions (see Fig. 6): at $x=0$, the component Z_3 obeys the same equation as in the bulk,

$$Z_3(0,y;L+2) = [UZ_+(L)]_3(0,y), \tag{16}$$

while the component Z_1 satisfies

$$Z_1(0,y;L+2) = -e^{i[\phi_1(0,y)+\phi_4(0,y)]} Z_3(0,y,L). \tag{17}$$

We wish to check under what conditions the evolution operator U has an eigenvector **u** representing an edge state. We simplify the discussion by considering a semi-infinite system without disorder, setting $\phi_i = 0$ for all i. Without disorder,

the spatial dependence, for $x \geqslant 1$, of such an eigenvector is $\mathbf{u}^{\top}(x,y)=(v,w)e^{(iqy-\lambda x)}$, where $\mathrm{Re}[\lambda]>0$; for $x=0$, $\mathbf{u}^{\top}(0,y)=(v',w')e^{iqy}$, where v,v',w, and w' are constants. This ansatz in the equation

$$U\mathbf{u}=e^{i\chi}\mathbf{u}, \tag{18}$$

taking U from Eqs. (7), (16), and (17), yields

$$e^{\lambda}=\tan\beta \tag{19}$$

confirming that an edge state exists ($\mathrm{Re}[\lambda]>0$) only for $\beta>\beta_c\equiv\pi/4$.

Similar results also follow if one considers directly the continuum limit. Let the eigenfunctions of $\widetilde{H}$ be $\widetilde{\Psi}(x,y)$, so that those of H are $\Psi(x,y)$, with $\Psi\equiv G\widetilde{\Psi}$. Writing $\Psi^{\top}=(\Psi_1,\Psi_3)$, the boundary condition at $x=0$, Eq. (17), is to leading order

$$\Psi_3(0,y)=i\Psi_1(0,y). \tag{20}$$

Note that this boundary condition enforces a chiral edge current: the current density, with components $j_{\alpha}=\Psi^{\dagger}\sigma_{\alpha}\Psi$, is $\mathbf{j}=(0,|\Psi_1|^2)$, and necessarily in the positive y direction. Imposing this boundary condition, the Dirac Hamiltonian H of Eq. (14) with $V=0$ and $\mathbf{A}=\mathbf{0}$ has an eigenfunction of energy E

$$\Psi(x,y)=e^{iEy}e^{-mx}\begin{pmatrix}1\\ i\end{pmatrix} \tag{21}$$

provided that $m>0$. This same eigenstate appears from considering an infinite system with position-dependent mass, $m(x,y)$, following Ludwig *et al.*: setting $m(x,y)=m$ for $x>0$, and $m(x,y)=m_0$ for $x<0$, the boundary condition, Eq. (20), emerges in the limit $m_0\to-\infty$.

IV. MAPPING FROM THE NETWORK MODEL TO A TIGHT-BINDING MODEL

It is also possible, without taking a continuum limit, to associate a nearest-neighbor tight-binding Hamiltonian with the network model. The sites of the tight-binding model, each carrying one basis state, correspond to the links of the network model. In terms of the one-step evolution matrix T the tight-binding Hamiltonian $\mathcal{H}$ is simply

$$\mathcal{H}=(T^{\dagger}-T)/i. \tag{22}$$

We indicate schematically in Fig. 7 which matrix elements of $\mathcal{H}$ are nonzero, and give their values in terms of link phases and the tunneling parameter.

This Hamiltonian has two important features. First, it is natural to introduce a unit cell containing the four sites arising from one plaquette of the network model. The amplitudes of nearest-neighbor hopping *within* and *between* unit cells have moduli $\cos\beta$ and $\sin\beta$, respectively, where β is the tunneling parameter: they are different, except at the critical point, $\beta=\beta_c\equiv\pi/4$. Second, the phases of the hopping matrix elements are correlated in the way indicated in Fig. 7. It follows from known behavior of the network model that these correlations have unusual consequences for the tight-binding model. Consider a system in which all link phases are independently and uniformly distributed. It is straightforward to see that for this system the eigenvalues of T in the complex plane are distributed uniformly on the unit circle. As a result, the density, $\rho(E)$, of eigenvalues E of $\mathcal{H}$ can be given exactly: $\rho(E)=\frac{1}{4}\pi[1-(E/2)^2]^{1/2}$ for $(E/2)^2\leqslant 1$ and $\rho(E)=0$ for $(E/2)^2>1$. In addition, one can see that the eigenvectors of T have the same statistical properties throughout the spectrum, a feature inherited by $\mathcal{H}$. Hence the localization length of eigenstates of $\mathcal{H}$ is independent of their energy E. If all nodes have the same parameter value, β, then as $\beta\to\beta_c$, the localization length diverges uniformly across the spectrum: this Hamiltonian never has a mobility edge as a function of energy.

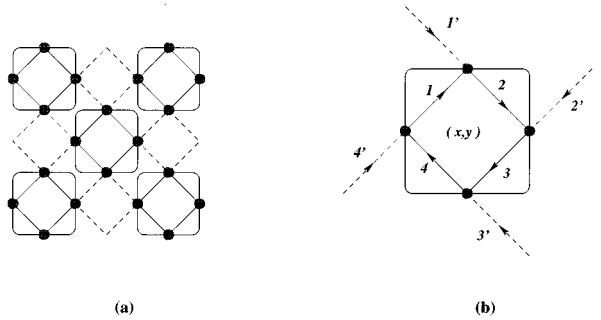

FIG. 7. Schematic illustration of the tight-binding Hamiltonian. (a) The only nonzero matrix elements are those linking nearest-neighbor sites, within plaquettes (full lines) and between plaquettes (dashed lines). (b) Their values are $ie^{i\phi_l(x,y)}\cos\beta$ for the bonds marked $l=1,2,3,4$, $ie^{i\phi_l(x,y)}\sin\beta$, for the bonds marked $l=1',2'$, and $-ie^{i\phi_l(x,y)}\sin\beta$, for the bonds marked $l=3',4'$, hopping in all cases being in the direction given by the arrows.

We note that $\mathcal{H}$ is similar in structure to, but different in detail from, the tight-binding model used as a departure point by Ludwig and collaborators.[9] The latter includes not only nearest-neighbor, but also next-nearest-neighbor hopping: compare Fig. 7 with Fig. 1 of Ref. 9. Our model also differs from that of Fisher and Fradkin.[13]

V. SUMMARY

We have set out in detail a mapping from the network model for plateau transitions in the IQHE to Dirac fermions in two space dimensions. The mapping makes crucial use of a unitary operator defined for the network model,[19] which is essentially the time-evolution operator. The two-component structure of Dirac spinors in two space dimensions arises rather naturally from the network model, defined on a square lattice: the fact that each plaquette has four sides suggests a four-component wave function, which separates into two independent pairs because of the existence of two sublattices. This structure is not dependent on the continuum limit, and is also shared by a nearest-neighbor tight-binding Hamiltonian, derived directly from the evolution operator.

ACKNOWLEDGMENT

This work was supported in part by EPSRC Grant No. GR/Go 2727 and by an ORS award to C.-M.H. from the CVCP.

[1] For reviews, see B. Hukenstein, Rev. Mod. Phys. **67**, 357 (1995); M. Janssen, O. Viehweger, U. Fastenrath, and J. Hajdu, *Introduction to the Theory of the Integer Quantum Hall Effect*, edited by J. Hajdu (VCH, Weinheim, 1994); and *The Quantum Hall Effect*, 2nd ed., edited by R.E. Prange and S.M. Girvin (Springer, Berlin, 1990).

[2] D.E. Khmel'nitskii, Pis'ma Zh. Éksp. Teor. Fiz. **38**, 454 (1983) [JETP Lett. **38**, 552 (1983)].

[3] H.P. Wei, D.C. Tsui, M.A. Paalanen, and A.M.M. Pruisken, Phys. Rev. Lett. **61**, 1294 (1988); S. Koch, R.J. Haug, K. von Klitzing, and K. Ploog, *ibid*. **67**, 883 (1991); L.W. Engel, D. Shahar, C. Kurdak, and D.C. Tsui, *ibid*. **71**, 2638 (1993).

[4] H. Levine, S.B. Libby, and A.M.M. Pruisken, Phys. Rev. Lett. **51**, 1915 (1983).

[5] N. Read (unpublished).

[6] D.-H. Lee, Phys. Rev. B **50**, 10 788 (1994).

[7] M.R. Zirnbauer, Ann. Phys. (Leipzig) **3**, 513 (1994).

[8] D.-H. Lee and Z. Wang, Philos. Mag. Lett. **73**, 145 (1996).

[9] A.W.W. Ludwig, M.P.A. Fisher, R. Shankar, and G. Grinstein, Phys. Rev. B **50**, 7526 (1994).

[10] For an illuminating discussion of the semiclassical limit, see M.V. Berry and R.J. Mondragon, Proc. R. Soc. London A **412**, 53 (1987).

[11] A.A. Nersesyan, A.M. Tsvelik, and F. Wenger, Phys. Rev. Lett. **72**, 2628 (1994); Nucl. Phys. **B438**, 561 (1995); D. Bernard, *ibid*. **B441**, 471 (1995); C. Mudry, C. Chamon, and X.-G. Wen, *ibid.* C. Chamon, C. Mudry, and X.-G. Wen (unpublished); J.-S. Caux, I.I. Kogan, and A.M. Tsvelik, *ibid.* **B466**, 444 (1996); I.I. Kogan, C. Mudry, and A.M. Tsvelik, Phys. Rev. Lett. **77**, 707 (1996).

[12] Y. Aharonov and A. Casher, Phys. Rev. A **19**, 2461 (1979).

[13] M.P.A. Fisher and E. Fradkin, Nucl. Phys. **B251**, 457 (1985).

[14] E. Fradkin, Phys. Rev. B **33**, 3257 (1986); **33**, 3263 (1986).

[15] K. Ziegler, Europhys. Lett. **28**, 549 (1994); **31**, 549 (1995).

[16] J.T. Chalker and P.D. Coddington, J. Phys. C **21**, 2665 (1988).

[17] D.-H. Lee, Z. Wang, and S.A. Kivelson, Phys. Rev. Lett. **70**, 4130 (1993); D.K.K. Lee and J.T. Chalker, *ibid.* **72**, 1510 (1994); Z.Q. Wang, D.-H. Lee, and X.G. Wen, *ibid.* **72**, 2454 (1994); V. Kagalovsky, B. Horovitz, and Y. Avishai, Phys. Rev. B **52**, 17 044 (1995); J.T. Chalker and A. Dohmen, Phys. Rev. Lett. **75**, 4496 (1995).

[18] H.A. Fertig and B.I. Halperin, Phys. Rev. B **36**, 7967 (1987).

[19] R. Klesse and M. Metzler, Europhys. Lett. **32**, 229 (1995).